A Spatial Filtering Based Gridless DOA Estimation Method for Coherent Sources

XIAOHUAN WU[1], (Member, IEEE), **WEI-PING ZHU**[2,3], (Senior Member, IEEE), **JUN YAN**[1], AND **ZEYUN ZHANG**[1]

[1]Key Lab of Broadband Wireless Communication and Sensor Network Technology, Nanjing University of Posts and Telecommunications, Nanjing 210003, China
[2]Department of Electrical and Computer Engineering, Concordia University, Montreal, QC H3G 1M8, Canada
[3]School of Communication and Information Engineering, Nanjing University of Posts and Telecommunications, Nanjing 210003, China

Corresponding author: Xiaohuan Wu (xiaohuanwu@njupt.edu.cn)

ABSTRACT In this paper, we investigate a covariance matrix reconstruction approach (CMRA) for direction-of-arrival (DOA) estimation in correlated/coherent sources scenario. We incorporate a spatial filtering (SF) model into our recently developed method CMRA in order to enhance its adaptation ability. In particular, a sliding window scheme is proposed to estimate the number of sources, and an iterative procedure is provided to estimate the DOAs of the signals. Since the original CMRA provides inaccurate estimate of the noise power which is undesirable during iterations, a new update rule for the noise power is proposed. Moreover, we derive a fast implementation of the SF-CMRA to accelerate the DOA estimation in each iteration. The proposed methods are suitable for both uniform and sparse linear arrays and are able to provide accurate estimates of DOAs, signal powers, and noise power. We also show that the proposed algorithmic framework can be easily extended to other gridless DOA estimation methods for accuracy improvement. Simulation results are provided to illustrate the superiority of our proposed methods.

INDEX TERMS DOA estimation, gridless methods, Toeplitz structure, coherent sources.

I. INTRODUCTION

Direction-of-arrival (DOA) estimation is one of the most important techniques in array signal processing and is employed in many applications, e.g., channel estimation [1] and tracking [2], [3]. Many DOA estimation methods have been proposed including the well known Capon method and subspace-based methods like MUSIC [4] and ESPRIT [5]–[7] (see [8] for a detailed review). However, these methods may have difficulties when the impinging signals are coherent or highly correlated. As such, many of these methods have employed the spatial smoothing (SS) method [9] to address this issue, which, however, require shift invariance property in the array and hence is applicable only for the uniform linear array (ULA) case [10]–[13].

Compressive sensing [14] is a technique of reconstructing a high dimensional signal from fewer samples and has been introduced into the DOA estimation area in the past decade, resulting in a number of sparse methods for DOA estimation [15]–[17]. Compared to the subspace-based methods, the sparse methods enjoy several advantages such as super-resolution, robustness to noise and immune to the source number. Since the sparse methods do not depend on the orthogonality between the noise and signal spaces which is sensitive to the correlation of the sources, they are often immune to the correlation. However, the sparse methods require the DOAs of interest to be sparse in the whole angle space. To this end, We discretize the angle space into a finite set of grid points and the DOAs of interest are further assumed to lie exactly on the grids. In fact, the DOAs lie in the continuous infinite set of angles, hence the assumption holds only when the size of the set tends to infinity, which results in an unacceptable computational cost. Moreover, The discretization may deteriorate the performance of the sparse methods since there always exists a bias between the DOAs and the grids, and we interpret it as a basis mismatch issue. Several modified off-grid methods have been proposed to address this issue [18]–[20]. However, these methods cannot eliminate the basis mismatch problem but may increase the computational cost [21].

Recently, by exploring the particular properties of the covariance matrix, the covariance matching criteria and the atomic norm techniques are employed to totally eliminate

the basis mismatch effect, resulting in two representative methods: sparse and parametric approcah (SPA) [21] and atomic norm minimization (ANM) [22]. Although SPA is proposed by assuming uncorrelated sources, it is shown to be related to the ℓ_1-norm minimzation problem and hence is robust to the correlation between the source signals [21]. ANM is proposed based on the atomic norm and can be also related to SPA. The equivalence between SPA and ANM is discussed in detail in [23]. Nevertheless, as we have shown in simulations, although SPA (or ANM) is able to identify the correlated sources, the estimation accuracy of SPA (or ANM) in highly correlated or even coherent sources scenario is still not satisfactory, making it unattractive in many applications. For instance, in channel estimation of massive multiple-input and multiple-output (MIMO) communications where the potential gains of massive MIMO systems rely heavily on the accuracy of channel estimation. The received signals from different paths may highly correlated, hence the inaccuracy of the estimates can lead to significant reduction of throughput.

By employing the covariance matching criterion, we have proposed a super-resolution method called covariance matrix reconstruction approach (CMRA) [24], [25] which can be applied for both the ULA and the sparse linear array (SLA). More importantly, discretizing the whole spatial space can be avoided. Hence, CMRA is immune to the basis mismatch effect. Nevertheless, CMRA also faces difficulties in the highly correlated or even coherent source scenarios. Moreover, unlike in the uncorrelated sources scenario, CMRA fails to give accurate estimates of the source powers in the case of coherent sources.

In this paper, we aim to enhance the adaptation ability of our original CMRA in the scenario where the sources are coherent. We first present a sliding window scheme to estimate the number of sources. Then, by incorporating the spatial filtering (SF) model into original CMRA, we separate the correlated sources model into several single DOA estimation models and propose an iterative procedure to estimate the DOAs. In addition, the signal and noise powers can be also estimated. Furthermore, since solving the optimization problem in each iteration of SF-CMRA is time-consuming, we simplify the constraints when the number of snapshots is medium or high and then propose a fast implementation of SF-CMRA. Compared to the original CMRA algorithm, the SF-CMRA and its fast implementation are able to provide satisfying estimation performance in the correlated/coherent scenarios, as will be shown in simulations. Finally, we show that our proposed algorithmic framework is also suitable for other gridless methods such as SPA for performance improvement.

The notations are privided below. $\mathbb{C}$ is the set of complex numbers. For a matrix A, the notations $\overline{A}$, A^T, A^H and $A^\dagger$ denote the conjugate, transpose, conjugate transpose and pseudo-inverse of A, respectively. $A \otimes B$ denotes the Kronecker product of matrices A and B. $A \geq 0$ means that matrix A is positive semidefinite. $A_{m,n}$ denotes the (m, n)-th entry of matrix A.

The organization of the paper is as follows. Section II introduces the signal model and the original CMRA method as preliminaries. Section III first proposes the SF-CMRA to improve the estimation performance of CMRA in the correlated sources scenario, and then derives a fast algorithm implementation to speed up the DOA estimation in each iteration. Simulations results are provided in Section IV to demonstrate the superiority of our methods. Conclusions are summarized in Section V.

II. PRELIMINARIES

A. SIGNAL MODEL

In this paper, we consider two array geometries: ULA and SLA. In the ULA case, we set the inter-element spacing to half-wavelength and define its sensor index set as $\{1, \cdots, N\}$, where N denotes the number of sensors. In the SLA case, we denote the sensor index set as $\boldsymbol{\Omega} = \{\Omega_1, \cdots, \Omega_M\}$, where $\boldsymbol{\Omega}$ is sorted in ascending order with $\Omega_1 = 1$, $\Omega_M = N$, in which $N \geq M$. Although the CMRA method is suitable for both the ULA and SLA, without loss of generality, only the SLA case is considered in the rest of this paper. But, we will take the ULA case into consideration in the simulation section.

Suppose K narrowband sources impinge onto an M-element SLA from $\boldsymbol{\theta} = \{\theta_1, \cdots, \theta_K\}$ simultaneously. The array output with L snapshots is,

$$X_{\boldsymbol{\Omega}} = \sum_{k=1}^{K} a_{\boldsymbol{\Omega}}(\theta_k) s_k + V = A_{\boldsymbol{\Omega}} S + V, \quad (1)$$

where $X_{\boldsymbol{\Omega}} \in \mathbb{C}^{M \times L}$ denotes the array output, $S = [s_1^T, \cdots, s_K^T]^T \in \mathbb{C}^{K \times L}$ is the impinged signal with s_k being the k-th signal, $A_{\boldsymbol{\Omega}} = [a_{\boldsymbol{\Omega}}(\theta_1), \cdots, a_{\boldsymbol{\Omega}}(\theta_K)]$ is the manifold with $a_{\boldsymbol{\Omega}}(\theta_k) = [e^{j\phi_{k,\Omega_1}}, \cdots, e^{j\phi_{k,\Omega_M}}]^T$ being the steering vector, and $V \in \mathbb{C}^{M \times L}$ is the additive white Gaussian noise. The manifold matrix of the coarray of the SLA can be defined as $A = [a(\theta_1), \cdots, a(\theta_K)]$ with $a(\theta_k) = [e^{j\phi_{k,1}}, \cdots, e^{j\phi_{k,N}}]^T$. The relationship between $a(\theta_k)$ and $a_{\boldsymbol{\Omega}}(\theta_k)$ can be formulated as $a_{\boldsymbol{\Omega}}(\theta_k) = \boldsymbol{\Gamma}_{\boldsymbol{\Omega}} a(\theta_k)$ where $\boldsymbol{\Gamma}_{\boldsymbol{\Omega}} \in \{0, 1\}^{M \times N}$ denotes a selection matrix with its entries being 1 only at (m, Ω_m) position.

B. CMRA

First, it is assumed that both the sources and the noise are uncorrelated from each other. By denoting the signal and the noise powers as $\boldsymbol{p} = [p_1, \cdots, p_K]^T$ and σ, respectively, the covariance matrix can be written as,

$$\begin{aligned}
R_{\boldsymbol{\Omega}} &= E[X_{\boldsymbol{\Omega}} X_{\boldsymbol{\Omega}}^H] \\
&= \sum_{k=1}^{K} p_k a_{\boldsymbol{\Omega}}(\theta_k) a_{\boldsymbol{\Omega}}^H(\theta_k) + \sigma I \\
&= T_{\boldsymbol{\Omega}}(\boldsymbol{u}) + \sigma I \\
&= \boldsymbol{\Gamma}_{\boldsymbol{\Omega}} T(\boldsymbol{u}) \boldsymbol{\Gamma}_{\boldsymbol{\Omega}}^T + \sigma I, \quad (2)
\end{aligned}$$

where $T_{\Omega}(u) \triangleq \Gamma_{\Omega} T(u) \Gamma_{\Omega}^T = A_{\Omega} \text{diag}(p) A_{\Omega}^H$ in which $T(u)$ is a Toeplitz matrix. Its structure can be given as follows:

$$T(u) = \begin{bmatrix} u_1 & u_2^* & \cdots & u_N^* \\ u_2 & u_1 & \cdots & u_{N-1}^* \\ \vdots & \vdots & \ddots & \vdots \\ u_N & u_{N-1} & \cdots & u_1 \end{bmatrix}. \qquad (3)$$

Note that $T(u)$ is uniquely determined by its first column $u = [u_1, \cdots, u_N]^T$. It is also clear that $\text{rank}[T(u)] = K < N$ and $T(u) \geq 0$.

In reality, R_{Ω} is usually obtained as follows,

$$\widehat{R}_{\Omega} = \frac{1}{L} X_{\Omega} X_{\Omega}^H, \qquad (4)$$

where L denotes the number of snapshots and $\widehat{R}$ is contaminated due to the finite snapshot effect. The error component can be denoted as

$$\begin{aligned} E_{\Omega} &= \widehat{R}_{\Omega} - R_{\Omega} \\ &= \widehat{R}_{\Omega} - T_{\Omega}(u) - \sigma I, \end{aligned} \qquad (5)$$

The vectorization form of E_{Ω} obeys the following asymptotic normal distribution [26],

$$\text{vec}(E_{\Omega}) \sim \text{AsN}(0, W_{\Omega}) \qquad (6)$$

where $W_{\Omega} = \frac{1}{L} R_{\Omega}^T \otimes R_{\Omega}$ and can be estimated as $\widehat{W}_{\Omega} = \frac{1}{L} \widehat{R}_{\Omega}^T \otimes \widehat{R}_{\Omega}$. From (6), it can be deduced that [27],

$$\left\| \widehat{W}_{\Omega}^{-\frac{1}{2}} \text{vec}(E_{\Omega}) \right\|_2^2 \sim \text{As}\chi^2(M^2), \qquad (7)$$

where $\text{As}\chi^2(M^2)$ denotes the asymptotic chi-square distribution with M^2 degrees of freedom. It is easy to see that the following inequality holds with probability $1 - \kappa$,[1]

$$\left\| \widehat{W}_{\Omega}^{-\frac{1}{2}} \text{vec}(E_{\Omega}) \right\|_2^2 \leq \eta^2 \qquad (8)$$

where η can be determined by M and κ.[2]

CMRA first estimates $T(u)$ which contains the DOA information by solving the following problem,

$$\begin{aligned} \min_{u} \quad & \text{tr}\,[T(u)] \\ \text{s.t.} \quad & \left\| \widehat{W}_{\Omega}^{-\frac{1}{2}} \text{vec}(E_{\Omega}) \right\|_2^2 \leq \eta^2, \\ & T(u) \geq 0. \end{aligned} \qquad (9)$$

Several toolboxes can be used to solve this problem, e.g., CVX and SeDuMi [28]. When the estimate $T(\widehat{u})$ is estimated, $\widehat{\theta}$ and $\widehat{p}$ can be retrieved according to the Vandermonde decomposition theorem (see [29] for more details).

It can be seen that CMRA requires the sources to be uncorrelated. Otherwise if the sources are correlated, the signal space of the covariance R_{Ω} is rank deficient and then

---

[1] In this paper, we set $\kappa = 0.0001$.
[2] According to the property of chi-square distribution, given the explicit value of M and κ, we can obtain η by using the MATLAB routine chi2inv$(1 - \kappa, M^2)$.

equation (2) is invalid. In turn, solving problem (8) may fail as well. The preprocessing techniques spatial smoothing has been proposed to solve the rank deficiency issue by exploiting the shift invariance property of the ULA [30]. However, spatial smoothing cannot be used in the SLA case, which may limit the adaptability of CMRA. Moreover, even though those techniques can help CMRA to deal with the correlated scenario, they perform poorly when the covariance matrix and subspace estimates are not accurate typically in cases like low signal-to-noise ratio (SNR) and spatially adjacent sources. The spatial filtering model was proposed by Liu *et al.* for the sparse DOA estimation model [31]. However, it has not yet been exploited for the gridless DOA estimation model. In next section, we will extend the SF model for CMRA and propose a unified algorithmic framework that is suitable for general gridless DOA estimation approaches.

III. SPATIAL FILTERING CMRA
A. SPATIAL FILTERING MODEL
Here, we first briefly review the SF model and then incorporate it into CMRA for performance improvement. Denote the manifold matrix of the subarray which consists of the m-th to $(m + K - 1)$-th elements of the original array with sources impinging from directions of θ by $A^{(m)}(\theta)$, and also define $B^{(m)}(\theta) = [A^{(m)}(\theta)]^{-1}$, with its k-th row denoted by $b_k^{(m)}$. Then, we get

$$\begin{aligned} B^{(m)}(\theta) A^{(m)}(\theta) S &= \Phi_m S, \quad m = 1, \cdots, M - K + 1, \\ b_k^{(m)} A^{(m)}(\theta) S &= e^{j\phi_{k,m}} s_k, \quad k = 1, \cdots, K, \end{aligned} \qquad (10)$$

where $\Phi_m = \text{diag}([e^{j\phi_{1,m}}, \cdots, e^{j\phi_{K,m}}])$. By defining $F_k \in \mathbb{C}^{(M-K+1)\times M}$, whose m-th row is

$$(F_k)_{m\bullet} = [0_{m-1}, b_k^{(m)}, 0_{M-K+1-m}], \qquad (11)$$

we have,

$$\begin{aligned} Y_k &\triangleq F_k X_{\Omega} \\ &= a'(\theta_k) s_k + F_k V, \quad k = 1, \cdots, K, \end{aligned} \qquad (12)$$

where $a'(\theta_k) = [e^{j\phi_{k,\Omega_1}}, \cdots, e^{j\phi_{k,\Omega_{N'}}}]$ is denoted as a_k for simplicity with $N' = M - K + 1$. We can see that the k-th signal is extracted from the array output and its DOA can be retrieved from model (12) provided that the spatial filter F_k is accurate. However, this model cannot be directly utilized for CMRA because of two reasons. First, the number of sources has to be required, which is usually *a priori* unknown. Second, the filter parameters depend on the true DOAs θ, which are not available in practice. In what follows, we first present a sliding window scheme to estimate K, and then propose an iterative procedure to jointly estimate the DOAs and the filter parameters.

B. SF-CMRA
Here, we introduce a sliding window scheme to estimate K. In particular, we employ the sparse and parametric

approach (SPA) to give an initialization of $\boldsymbol{\theta}$ and $\widehat{K}$.[3] The SPA output $\widehat{\boldsymbol{p}} = [\widehat{p}_1, \cdots, \widehat{p}_{N-1}]^T$ is sorted in deceasing order where $\{\widehat{p}_k, k \leq K\}$ are the true signal powers and $\{\widehat{p}_k, k > K\}$ are the spurious ones. Let $b_k = \sum_{m=1}^{\mathcal{K}} \widehat{p}_{m+k-1}(k = 1, \cdots, N - \mathcal{K} - 1)$, where $\mathcal{K}$ denotes the window size. Note that there exists a noticeable gap between $\widehat{p}_K$ and $\widehat{p}_{K+1}$, hence $\frac{b_k}{b_{k+1}}$ approaches the maximum value when $k = K$. Hence, the signal number can be estimated as

$$\widehat{K} = \arg\max_k \frac{b_k}{b_{k+1}} \quad k = 1, \cdots, N - \mathcal{K} - 1. \quad (13)$$

In this paper, the window size $\mathcal{K}$ is set to 1. It is noted that a similar sliding window scheme in [32] sets $\mathcal{K} = 2$. However, the choice of $\mathcal{K} = 1$ allows to locate $N - 2$ sources while the scheme in [32] and [33] using $\mathcal{K} = 2$ can locate $N - 3$ sources only. Hence, in this paper, we choose $\mathcal{K} = 1$ for source enumeration.

For DOA estimation, we propose an iterative procedure to update θ_k and $\boldsymbol{F}_k$ alternatively, where $\boldsymbol{F}_k$ is estimated by (11). The remaining task is to estimate θ_k based on (12). Note that model (12) can be regarded as an SLA model when the original array is sparse. Here, we only consider the SLA case in the following and have,

$$\boldsymbol{R}_{Y_k}^{(q)} = \boldsymbol{T}_{\boldsymbol{\Omega}'}(\boldsymbol{u}_k^{(q)}) + \sigma^{(q)}\boldsymbol{F}_k^{(q)}(\boldsymbol{F}_k^{(q)})^H, \quad (14)$$

where $^{(q)}$ is used to identify the updating variables in the q-th iteration, $\boldsymbol{R}_{Y_k}$ is the covariance matrix of $\boldsymbol{Y}_k$ and $\boldsymbol{T}_{\boldsymbol{\Omega}'}(\boldsymbol{u}_k) = \boldsymbol{\Gamma}_{\boldsymbol{\Omega}'}\boldsymbol{T}(\boldsymbol{u}_k)\boldsymbol{\Gamma}_{\boldsymbol{\Omega}'}^H$ in which $\boldsymbol{\Gamma}_{\boldsymbol{\Omega}'}$ is the selection matrix of an array with $\boldsymbol{\Omega}' = \{\Omega_1, \cdots, \Omega_{N'}\}$. Before employing CMRA to reconstruct $\boldsymbol{T}_{\boldsymbol{\Omega}'}(\boldsymbol{u}_k)$, the noise power σ should be accurately estimated in advance. To this end, we first use (12) to obtain,

$$\begin{aligned}
&\text{diag}\left[\sigma \boldsymbol{F}_k^{(q)}(\boldsymbol{F}_k^{(q)})^H\right] \\
&= \text{diag}\left[\frac{1}{L}\left(\boldsymbol{F}_k^{(q)}\boldsymbol{X}_{\boldsymbol{\Omega}} - \boldsymbol{a}_k^{(q)}\boldsymbol{a}_k^{(q)\dagger}\boldsymbol{F}_k^{(q)}\boldsymbol{X}_{\boldsymbol{\Omega}}\right)\right. \\
&\qquad\qquad \left.\times \left(\boldsymbol{F}_k^{(q)}\boldsymbol{X}_{\boldsymbol{\Omega}} - \boldsymbol{a}_k^{(q)}\boldsymbol{a}_k^{(q)\dagger}\boldsymbol{F}_k^{(q)}\boldsymbol{X}_{\boldsymbol{\Omega}}\right)^H\right] \\
&= \text{diag}\left[\left(\boldsymbol{I} - \boldsymbol{a}_k^{(q)}\boldsymbol{a}_k^{(q)\dagger}\right)\boldsymbol{F}_k^{(q)}\widehat{\boldsymbol{R}}_{\boldsymbol{\Omega}}(\boldsymbol{F}_k^{(q)})^H\right] \\
&\triangleq \text{diag}(\boldsymbol{D}_k^{(q)}). \quad (15)
\end{aligned}$$

Then, the update rule for σ can be formulated as,

$$\sigma_k^{(q)} = \frac{\text{tr}\left[\boldsymbol{D}_k^{(q)}\right]}{\text{tr}\left[\boldsymbol{F}_k^{(q)}(\boldsymbol{F}_k^{(q)})^H\right]}. \quad (16)$$

When the estimate of $\sigma_k^{(q)}$ is obtained, the remaining task is to estimate $\boldsymbol{u}_k^{(q)}$ by using CMRA. To this end, we solve the

---

[3]It should be noted that, although SPA is applicable to the correlated scenario, it cannot provide a satisfying estimation performance because of the high correlation between the sources. We further show in simulation that, with the help of our proposed algorithmic framework, the performance of SPA can be also greatly improved.

following optimization problem,

$$\min_{\boldsymbol{u}_k^{(q)}} \text{tr}\left[\boldsymbol{T}(\boldsymbol{u}_k^{(q)})\right]$$

$$\text{s.t.} \quad \left\|(\widehat{\boldsymbol{W}}_k^{(q)})^{-\frac{1}{2}}\text{vec}(\boldsymbol{E}_k^{(q)})\right\|_2^2 \leq \beta^2,$$

$$\boldsymbol{T}(\boldsymbol{u}_k^{(q)}) \geq \boldsymbol{0}, \quad (17)$$

where $\widehat{\boldsymbol{W}}_k^{(q)} = \frac{1}{L}\widehat{\boldsymbol{R}}_{Y_k}^{(q)}(\widehat{\boldsymbol{R}}_{Y_k}^{(q)})^H$, $\boldsymbol{E}_k^{(q)} = \widehat{\boldsymbol{R}}_{Y_k}^{(q)} - \boldsymbol{T}_{\boldsymbol{\Omega}'}(\boldsymbol{u}_k^{(q)}) - \sigma_k^{(q)}\boldsymbol{F}_k^{(q)}(\boldsymbol{F}_k^{(q)})^H$ and β is uniquely determined by N' and κ. When the estimate $\widehat{\boldsymbol{u}}_k^{(q)}$ is obtained, the DOAs $\widehat{\boldsymbol{\theta}}_k^{(q)}$ and signal powers $\widehat{\boldsymbol{p}}_k^{(q)}$ can be easily determined by using the Vandermonde decomposition lemma [21].

We summarize our method in Algorithm 1 below, whose advantages can be listed as follows.

- our proposed algorithmic framework can adapt to arbitrary linear arrays (e.g., ULAs and SLAs) for coherent sources localization. In contrast, the spatial smoothing method only adapts to the special geometries such as ULA.
- the proposed framework is not only suitable for CMRA, but also can be extended to other gridless methods like SPA. The only difference is to update $\boldsymbol{u}_k$ by SPA instead of CMRA.
- SF-CMRA can provide accurate estimates of multiple parameters, including $\boldsymbol{\theta}, \boldsymbol{p}$ and σ, while most of the DOA estimation methods provide the DOA estimates only.
- the estimation performance of our method is superior to the spatial smoothing method.

All of these aforementioned advantages will be verified in simulations.

Algorithm 1 SF-CMRA

Input: measurement data $\boldsymbol{X}_{\boldsymbol{\Omega}}$.
  Initialization: the SPA output $\widehat{\boldsymbol{\theta}}^{(0)}, \widehat{\boldsymbol{p}}^{(0)}$.
  obtain the estimate $\widehat{K}$ by using (13);
  repeat
    calculate $\boldsymbol{F}_k$, $k = 1, \cdots, \widehat{K}$ in model (12);
    for: $k = 1, \cdots, \widehat{K}$
      Update σ_k by using equation (16);
      Update $\boldsymbol{u}_k$ by using model (17);
      Update θ_k and p_k by using the Vandermonde decomposition lemma;
    end
  until Convergence
Output: $\widehat{\boldsymbol{\theta}}, \widehat{\boldsymbol{p}}, \widehat{\sigma}_k, \widehat{K}$.

Remark 1: It can be noted that the noise power σ is estimated in each SF model as $\widehat{\sigma}_k$. A reasonable estimate of σ can be calculated as $\widehat{\sigma} = \frac{1}{\widehat{K}}\sum_{k=1}^{\widehat{K}}\widehat{\sigma}_k$.

Remark 2: Model (12) is regarded as an SLA with $\boldsymbol{\Omega}' = \{\Omega_1, \cdots, \Omega_{N'}\}$, which is not necessarily a redundancy array since its coarray is not guaranteed to be a ULA. It is natural

to require $K < \overline{M}$ where $\overline{M}$ is the maximum number of detectable sources. Our model always satisfies this requirement since there exists only one signal in each SF model as shown in (12), hence SF-CMRA can be implemented straightforwardly. The computational complexity of SF-CMRA is inevitably high because of the optimization problem (17) in each iteration. Solving this semidefinite programming problem (17) involves employing the optimization toolboxes such as CVX [34] or SeDuMi, which are time-consuming. Hence, we would like to propose in the following a more efficient implementation for SF-CMRA.

C. FAST IMPLEMENTATION OF SF-CMRA

Our idea behind a fast implementation of SF-CMRA is to obtain a closed-form solution for the DOA estimation problem in each iteration. It is noted that, the covariance matrix $T(\boldsymbol{u}_k)$ in model (17) is constrained to be positive semidefinite, which is almost sure with moderate or large number of snapshots. The research in [35] suggests that $L \geq 15$ is large enough to ensure that the estimated covariance matrix is positive semidefinite. Under this assumption, we can drop the constraint $T(\boldsymbol{u}_k^{(q)}) \geq \boldsymbol{0}$ in (17), leading to a Lagrangian form of the optimization problem as given by,

$$\min_{\boldsymbol{u}_k^{(q)}} \lambda \mathrm{tr}\left[\boldsymbol{T}(\boldsymbol{u}_k^{(q)})\right] + \frac{1}{2}\left\|(\widehat{\boldsymbol{W}}_k^{(q)})^{-\frac{1}{2}}\mathrm{vec}(\boldsymbol{E}_k^{(q)})\right\|_2^2, \quad (18)$$

where $\lambda > 0$ is a user-defined regularization parameter. By defining $\boldsymbol{Q} = \widehat{\boldsymbol{W}}^{-\frac{1}{2}}$ and $\widehat{\boldsymbol{R}}_{-\sigma} = \widehat{\boldsymbol{R}}_Y - \sigma \boldsymbol{F}\boldsymbol{F}^H$, we can then rewrite model (18) as,[4]

$$\begin{aligned}\min_{\boldsymbol{u}} \ & \frac{1}{2}\left\|\boldsymbol{Q}\mathrm{vec}\left(\widehat{\boldsymbol{R}}_{-\sigma} - \boldsymbol{T}_{\boldsymbol{\Omega'}}(\boldsymbol{u})\right)\right\|_2^2 + \lambda\mathrm{tr}\left[\boldsymbol{T}(\boldsymbol{u})\right]\\ = \min_{\boldsymbol{u}} \ & \frac{1}{2}\left[\mathrm{tr}\left[\boldsymbol{T}_{\boldsymbol{\Omega'}}(\boldsymbol{u})\widehat{\boldsymbol{R}}_{-\sigma}^{-1}\boldsymbol{T}_{\boldsymbol{\Omega'}}(\boldsymbol{u})\widehat{\boldsymbol{R}}_{-\sigma}^{-1}\right] - 2\mathrm{tr}\left[\boldsymbol{T}_{\boldsymbol{\Omega'}}(\boldsymbol{u})\widehat{\boldsymbol{R}}_{-\sigma}\right]\right]\\ & + \lambda\mathrm{tr}\left[\boldsymbol{T}(\boldsymbol{u})\right]\\ = \min_{\boldsymbol{u}} \ & \frac{1}{2}\mathrm{tr}\left[\boldsymbol{T}(\boldsymbol{u})\boldsymbol{C}\boldsymbol{T}(\boldsymbol{u})\boldsymbol{C}\right] + \mathrm{tr}\left[(\lambda\boldsymbol{I} - \boldsymbol{C})\boldsymbol{T}(\boldsymbol{u})\right], \quad (19)\end{aligned}$$

where $\boldsymbol{C} = \boldsymbol{\Gamma}_{\boldsymbol{\Omega'}}^T \widehat{\boldsymbol{R}}_{-\sigma}^{-1} \boldsymbol{\Gamma}_{\boldsymbol{\Omega'}}$. By using the Karush-Kuhn-Tucker (KKT) conditions, the optimal value of (18) can be given as follows,

$$\boldsymbol{T}^*(\boldsymbol{C}\boldsymbol{T}(\boldsymbol{u})\boldsymbol{C}) = \boldsymbol{T}^*(\boldsymbol{C} - \lambda\boldsymbol{I}). \quad (20)$$

where $\boldsymbol{T}^*(\boldsymbol{V}) = [v_{-(N'-1)}, \cdots, v_{N'-1}]^T$, in which v_n is the sum of entries in the n-th diagonal of $\boldsymbol{V} \in \mathbb{C}^{N' \times N'}$ which is defined as,

$$v_n = \begin{cases} \sum_{i=0}^{N'-1-n} \boldsymbol{V}_{1+i,n+1+i} & n = 0, \cdots, N'-1 \\ \sum_{i=0}^{N'-1+n} \boldsymbol{V}_{1-n+i,1+i} & n = -(N'-1), \cdots, -1. \end{cases} \quad (21)$$

In the following, we will provide an easy-to-implement procedure to efficiently solve (20). First, the left-hand term

---

[4]We drop the superscript $^{(q)}$ and the subscript k for notational convenience.

of (20) can be transformed as,

$$\boldsymbol{T}^*(\boldsymbol{C}\boldsymbol{T}(\boldsymbol{u})\boldsymbol{C}) = \begin{bmatrix} \overline{\boldsymbol{\Phi}}_{N',:} \\ \vdots \\ \overline{\boldsymbol{\Phi}}_{2,:} \\ \boldsymbol{\Phi} \end{bmatrix} \begin{bmatrix} u_{N'} \\ \vdots \\ u_2 \\ \overline{\boldsymbol{u}} \end{bmatrix}, \quad (22)$$

where

$$\boldsymbol{\Phi} = \begin{bmatrix} \boldsymbol{T}^{*T}\left(\boldsymbol{C}_{:,\{1,\cdots,N'\}}\boldsymbol{C}_{\{1,\cdots,N'\},:}\right) \\ \boldsymbol{T}^{*T}\left(\boldsymbol{C}_{:,\{1,\cdots,N'-1\}}\boldsymbol{C}_{\{2,\cdots,N'\},:}\right) \\ \vdots \\ \boldsymbol{T}^{*T}\left(\boldsymbol{C}_{:,1}\boldsymbol{C}_{N',:}\right) \end{bmatrix}, \quad (23)$$

We then rewrite (22) as,

$$\begin{aligned}\boldsymbol{T}^*\left[\boldsymbol{C}\boldsymbol{T}(\boldsymbol{u})\boldsymbol{C}\right] &= \boldsymbol{Z}\begin{bmatrix}\boldsymbol{u} \\ \overline{\boldsymbol{u}}\end{bmatrix}\\ &= [\boldsymbol{Z}_1 \ \boldsymbol{Z}_2]\begin{bmatrix}\boldsymbol{u} \\ \overline{\boldsymbol{u}}\end{bmatrix}, \quad (24)\end{aligned}$$

where $\boldsymbol{Z}_1$ and $\boldsymbol{Z}_2$ have the same dimension. Let $\boldsymbol{G}$ denote the right-hand side of (20), we can have that,

$$\underbrace{\begin{bmatrix}\mathcal{R}(\boldsymbol{G}) \\ \mathcal{I}(\boldsymbol{G})\end{bmatrix}}_{\boldsymbol{G}_r} = \underbrace{\begin{bmatrix}\mathcal{R}(\boldsymbol{Z}_1 + \boldsymbol{Z}_2) & \mathcal{I}(\boldsymbol{Z}_2 - \boldsymbol{Z}_1) \\ \mathcal{I}(\boldsymbol{Z}_1 + \boldsymbol{Z}_2) & \mathcal{R}(\boldsymbol{Z}_1 - \boldsymbol{Z}_2)\end{bmatrix}}_{\boldsymbol{Z}_r} \underbrace{\begin{bmatrix}\mathcal{R}(\boldsymbol{u}) \\ \mathcal{I}(\boldsymbol{u})\end{bmatrix}}_{\boldsymbol{u}_r}. \quad (25)$$

It is seen from (25) that $\boldsymbol{u}$ can be easily obtained from $\boldsymbol{u}_r = \boldsymbol{Z}_r^\dagger \boldsymbol{G}_r$. Compared to using CVX, the derived closed-form solution can greatly save computations and is termed as fast SF-CMRA (FSF-CMRA). Its superiorities will be investigated in the following section.

IV. SIMULATION RESULTS

We carry out extensive simulations to illustrate the superiority of our methods SF-CMRA/FSF-CMRA compared to some state-of-the-art methods, i.e., ℓ_1 reconstruction after Singular Value Decomposition (L1SVD) [36], sparse iterative covariance-based estimation (SPICE) [37] and SPA in correlated/coherent sources scenario. Moreover, we also take CMRA with spatial smoothing preprocessing into consideration and name it as SS-CMRA. It should be noted that, SS-CMRA is applicable for the uncorrelated sources scenario only. The iteration in SF-CMRA stops if the maximum number of iterations, set to 20, is reached, or the relative change of $\widehat{\boldsymbol{\theta}}$ at two consecutive iterations is less than 10^{-4}, i.e., $\frac{\|\boldsymbol{\theta}_{j+1}-\boldsymbol{\theta}_j\|_F}{\|\boldsymbol{\theta}_j\|_F} < 10^{-4}$. For L1-SVD and SPICE, we set the discretized interval to be $2°$ and the iterative grid refinement procedure is employed [36]. The arrays employed in this paper include one ULA with 7 sensors and one SLA with $\boldsymbol{\Omega} = \{1, 2, 5, 7\}$.

A. CONVERGENCE OF SF-CMRA

First, we give an example to illustrate the iterative process of SF-CMRA. Assume two narrowband coherent signals with $\boldsymbol{p} = [100, 100]^T$ impinge onto the ULA from $[-10°, 10°]$,

and the noise power $\sigma = 1$. We collect 100 snapshots for SF-CMRA algorithm and show the DOA and power estimates in each iteration in Fig. 1. In the upper two figures, the green and red points denote the initialization and last outputs of SF-CMRA, respectively. Blue points denote the outputs of SF-CMRA during iterations (the arrows indicate the order of iterations), and black circles denote the true powers and DOAs of sources. The lower two figures show the RMSEs of the estimates of DOAs and signal powers, respectively. From Fig. 1 we can observe that our method SF-CMRA is able to converge to the true points, providing accurate estimates of DOAs and powers. In particular, the RMSEs of θ, p and σ are 0.0102°, 0.0883 and 0.1181, respectively.
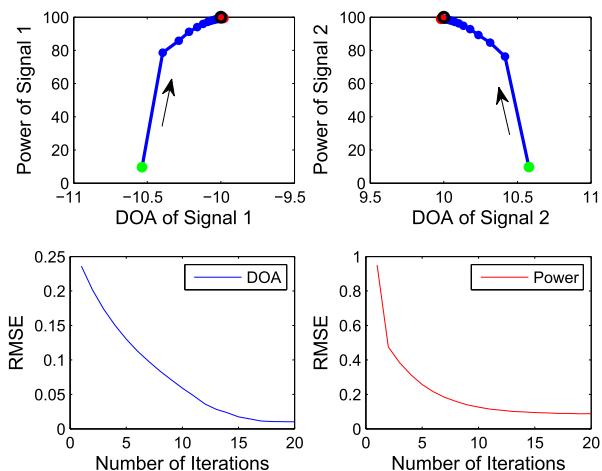
FIGURE 1. DOA and power estimates of SF-CMRA with $L = 100$, SNR $= 20$dB in the ULA case. The green and red points denote the initialization and last output of SF-CMRA, respectively. Blue points denote the outputs of SF-CMRA during iterations (the arrows indicate the order of iterations), and black circles denote the true positions of the signals.
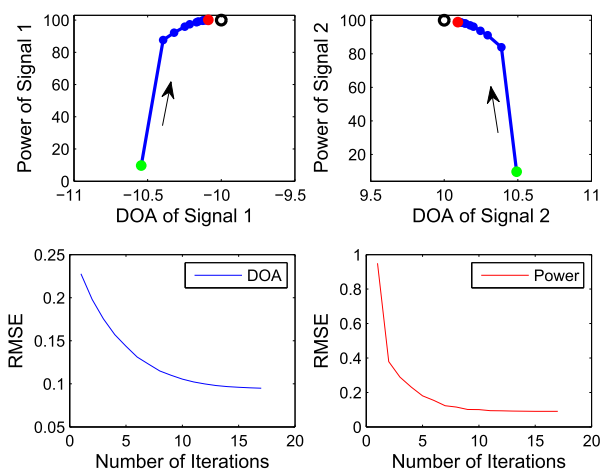

FIGURE 2. DOA and power estimates of SF-CMRA with $L = 100$, SNR $= 20$dB in the SLA case. The green and red points denote the initialization and last output of SF-CMRA, respectively. Blue points denote the outputs of SF-CMRA during iterations (the arrows indicate the order of iterations), and black circles denote the true DOAs and powers of signals.

Then, we re-implement the above experiment with the same settings except that we replace the ULA by the SLA and show the results in Fig. 2. It can be seen that SF-CMRA is applicable in the coherent sources scenario and is able to provide accurate estimates of both DOAs and signal powers.
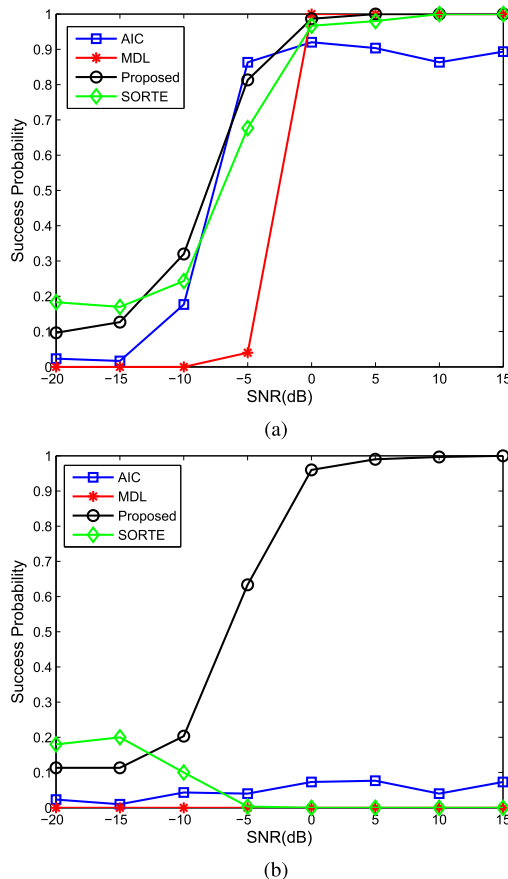

FIGURE 3. Detection probabilities comparison for two sources impinging from $[-6°, 6°]$, $L = 40$. (a) Uncorrelated sources. (b) Coherent sources.

In particular, the RMSEs of θ, p and σ are 0.0222°, 0.0913 and 0.1457, respectively.

B. COMPARISONS WITH PRIOR ARTS

We first evaluate the signal detection performance of our sliding window scheme by comparing with AIC, MDL as well as SORTE. Both the uncorrelated and coherent scenarios are considered. Assume two signals impinged onto the ULA from $[-6°, 6°]$ with $L = 40$. The success probabilities of the signal detection are measured in Fig. 3. From the left figure we can see that when the sources are uncorrelated, all methods can correctly detect the sources with high probabilities in the large SNR region and our sliding window scheme is able to give the best performance in most cases. However, when the sources are coherent, from the right figure we can observe that, only our method is able to correctly detect the sources with appropriate SNRs. Other methods failed when the sources are coherent since the covariance matrix may loss rank in this case.

We now evaluate the estimation performance of SF-CMRA by comparing the RMSEs of different methods with respect to SNR, L and correlation coefficient, respectively. First, we assume two coherent sources impinged onto the ULA from $[-16° + \nu, 16° + \nu]$ where ν is varied in each trial to simulate a realistic scenario. Assume that 100 snapshots are collected in each trial. We compare the estimation results
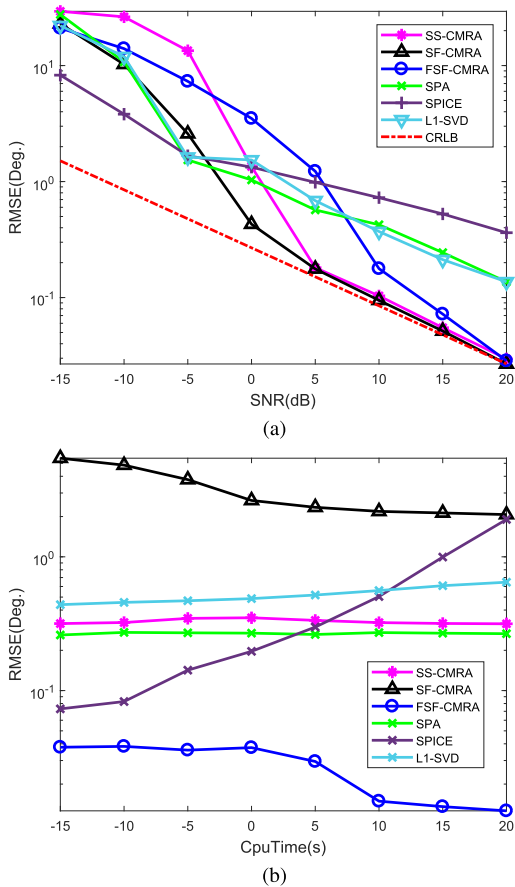
(a)

(b)

FIGURE 4. Performance comparison for two coherent sources impinging from $[-16° + v, 16° + v]$, $L = 100$. (a) RMSE comparison. (b) CPUtime comparison.

of the aforementioned methods based on 400 independent trials in Fig. 4 and vary the SNR from -15dB to 20dB. Fig. 4(a) and (b) show the RMSEs and CPU times of these methods, respectively. From Fig. 4(a) we can see that SF-CMRA enjoys the best estimation performance in most cases and follow the CRLB curve when SNR is larger than 5dB. With the help of spatial smoothing, SS-CMRA is able to give a satisfying performance in this experiment. Although the performance of FSF-CMRA is slightly inferior to that of SF-CMRA in the small/moderate SNR region (this is partially because we drop the nonnegative constraint), it can also follow CRLB when the SNR is large than 15dB. We also provide the running time comparisons in Fig. 4(b). SF-CMRA is time-consuming because it has to carry out the CVX toolbox to solve the optimization problem, which is computationally inefficient. The running times of SS-CMRA and SPA are comparable with each other and nearly remain stable in the compared SNR region. In contrast, the running times of L1SVD and SPICE increase as SNR becomes large since the grid size grows in proportion to the SNR. Thanks to the derived closed-form solution of problem (18), FSF-CMRA is more than an order of magnitude faster than other methods, making it more appealing in real applications.

We then evaluate the performance of these methods by varying L from 50 to 400 and setting SNR= 20dB.

The simulation results are given in Fig. 5, from which we can conclude that SF-CMRA is able to follow well the CRLB in the compared region. Although L1-SVD, SPICE and SPA are shown to be robust to the coherent sources [21], they fail to provide a satisfying performance in this experiment. In contrast, SS-CMRA and FSF-CMRA outperform L1-SVD, SPICE and SPA and have a similar trend as the CRLB.
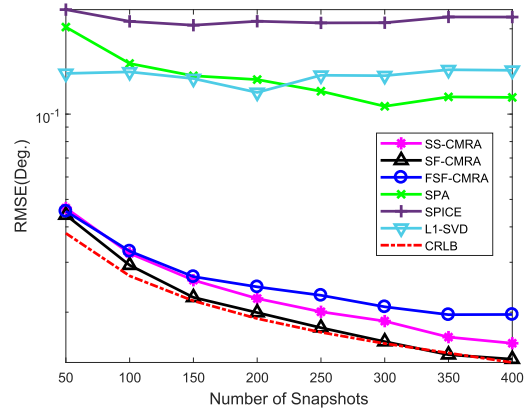

FIGURE 5. Performance comparison for two coherent sources impinging from $[-16° + v, 16° + v]$ with L varying from 50 to 400, SNR= 20dB.

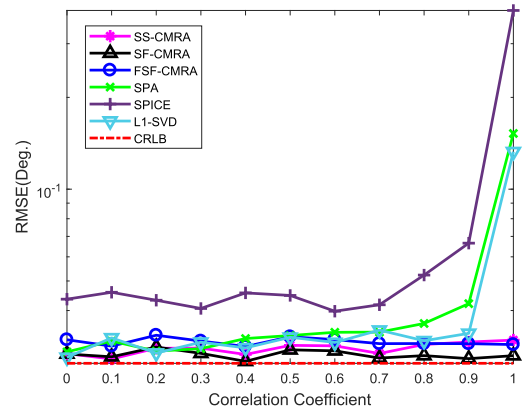**FIGURE 6.** Performance comparison for two correlated sources impinging from $[-16° + v, 16° + v]$ with correlation coefficient varying from 0 to 1, $L = 100$, SNR= 20dB.

Finally, we carry out simulation to evaluate the RMSEs with the correlation coefficient varying from 0 to 1 and set $L = 100$. The simulation results can be seen in Fig. 6. We can observe that the RMSEs of L1-SVD, SPICE and SPA increase when the two sources become correlated each other, especially when the two sources are coherent. In contrast, our proposed methods and SS-CMRA are immune to the correlation between the sources.

C. EXTENDABILITY OF SF-CMRA
We now show that our proposed framework can be easily extended to another gridless method SPA. In particular, we update u_k by SPA instead of CMRA in Algorithm 1 and name the proposed method as SF-SPA. Note that other gridless methods such as the proposed methods in [38] and [39] can also be incorporated into Algorithm 1 for performance
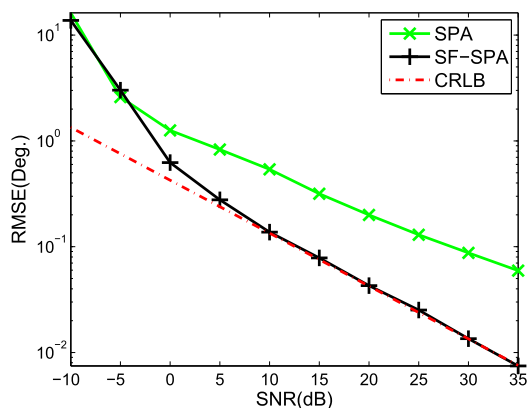
FIGURE 7. RMSE comparison of SPA and SF-SPA with respect to SNR with $N = 7$, $M = 4$, $L = 40$ for two coherent signals impinging from $[-16° + v, 16° + v]$.
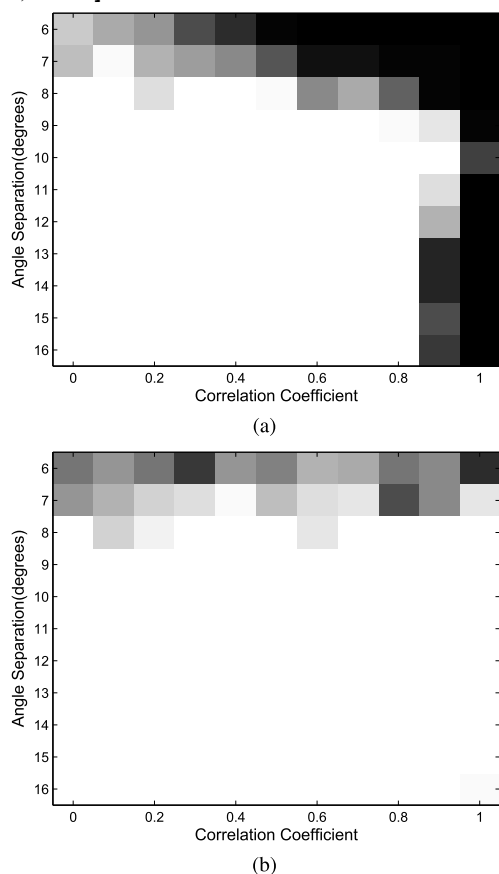

FIGURE 8. Estimation performance comparison of SPA and SF-SPA. (a) SPA. (b) SF-SPA.

improvement in the correlated sources scenario. We then evaluate the estimation performance of SPA and SF-SPA by comparing their RMSEs with respect to SNR. First, it is supposed that two coherent signals impinge onto the SLA from $[-16° + v, 16° + v]$. We set $L = 40$ and compare SPA and SF-SPA in Fig. 7. It is seen that the SF-SPA curve coincides with the CRLB curve while there still exist a noticeable gap between the SPA curve and the CRLB curve.

Finally, we study the estimation capabilities of SPA and SF-SPA in terms of the angle separation and correlation coefficient. We assume two signals impinge onto the ULA

from $[-3°, 3° + \Delta\theta]$, where $\Delta\theta$ varies from $0°$ to $10°$. In each Monte Carlo run, the SNR and L are set to 15dB and 100, respectively. Successful estimate is declared if the RMSE of DOA estimation is less than 0.1. The simulation results are presented in Fig. 8 where white means complete success and black means complete failure. It is obvious that SF-SPA has a larger success region compared to SPA. Moreover, Fig. 8 also shows that SPA suffers from high correlations even if the signals are well-separated while SF-SPA is insensitive to the correlations. From Fig. 7 and Fig. 8 it can be concluded that, the proposed framework can help gridless methods in general to improve their estimation performance in the correlated sources scenario.

V. CONCLUSIONS

In this paper, we have made a special effort to enhance the ability of the original CMRA algorithm in correlated/coherent sources scenario. By incorporating the SF model into CMRA, we have proposed a modified CMRA, called SF-CMRA method that uses a sliding window scheme to estimate the number of sources and an iterative procedure to estimate the DOAs. An update rule for the noise power is also provided. We have also derived an efficient algorithm, named FSF-CMRA, for fast implementation. Numerical results have revealed that the SF-CMRA is applicable in both ULA and SLA cases and is superior to other methods in estimation accuracy while FSF-CMRA enjoys a much lower computational complexity than other methods. We have also investigated the extendability of our proposed algorithmic framework revealing that other gridless methods can be easily incorporated into this framework to improve their estimation accuracy for correlated sources.

REFERENCES

[1] A. Alkhateeb, O. El Ayach, G. Leus, and R. W. Heath, Jr., "Channel estimation and hybrid precoding for millimeter wave cellular systems," *IEEE J. Sel. Topics Signal Process.*, vol. 8, no. 5, pp. 831–846, Oct. 2014.

[2] L. Wan, G. Han, L. Shu, S. Chan, and T. Zhu, "The application of DOA estimation approach in patient tracking systems with high patient density," *IEEE Trans. Ind. Inform.*, vol. 12, no. 6, pp. 2353–2364, Dec. 2016.

[3] L. Wan, X. Kong, and F. Xia, "Joint range-Doppler-angle estimation for intelligent tracking of moving aerial targets," *IEEE Internet Things J.*, vol. 5, no. 3, pp. 1625–1636, Jun. 2018, doi: 10.1109/JIOT.2017.2787785.

[4] R. O. Schmidt, "Multiple emitter location and signal parameter estimation," *IEEE Trans. Antennas Propag.*, vol. AP-34, no. 3, pp. 276–280, Mar. 1986.

[5] R. Roy and T. Kailath, "Esprit-estimation of signal parameters via rotational invariance techniques," *IEEE Trans. Acoust., Speech, Signal Process.*, vol. 37, no. 7, pp. 984–995, Jul. 1989.

[6] C. Zhou, Y. Gu, Z. Shi, and Y. D. Zhang, "Off-grid direction-of-arrival estimation using coprime array interpolation," *IEEE Signal Process. Lett.*, to be published, doi: 10.1109/LSP.2018.2872400.

[7] H. Chen *et al.*, "Esprit-like two-dimensional direction finding for mixed circular and strictly noncircular sources based on joint diagonalization," *Signal Process.*, vol. 141, pp. 48–56, Dec. 2017.

[8] H. Krim and M. Viberg, "Two decades of array signal processing research: The parametric approach," *IEEE Signal Process. Mag.*, vol. 13, no. 4, pp. 67–94, Jul. 1996.

[9] S. U. Pillai and B. H. Kwon, "Forward/backward spatial smoothing techniques for coherent signal identification," *IEEE Trans. Acoust., Speech Signal Process.*, vol. 37, no. 1, pp. 8–15, Jan. 1989.

[10] A. Moghaddamjoo, "Application of spatial filters to DOA estimation of coherent sources," *IEEE Trans. Signal Process.*, vol. 39, no. 1, pp. 221–224, Jan. 1991.

[11] H. Chen, C. Hou, W. Liu, W.-P. Zhu, and M. N. S. Swamy, "Efficient two-dimensional direction-of-arrival estimation for a mixture of circular and noncircular sources," *IEEE Sensors J.*, vol. 16, no. 8, pp. 2527–2536, Apr. 2016.

[12] H. Chen, C.-P. Hou, Q. Wang, L. Huang, and W.-Q. Yan, "Cumulants-based Toeplitz matrices reconstruction method for 2-D coherent doa estimation," *IEEE Sensors J.*, vol. 14, no. 8, pp. 2824–2832, Aug. 2014.

[13] Y. Gu and A. Leshem, "Robust adaptive beamforming based on interference covariance matrix reconstruction and steering vector estimation," *IEEE Trans. Signal Process.*, vol. 60, no. 7, pp. 3881–3885, Jul. 2012.

[14] D. L. Donoho, "Compressed sensing," *IEEE Trans. Inf. Theory*, vol. 52, no. 4, pp. 1289–1306, Apr. 2006.

[15] C. Zhou, Y. Gu, X. Fan, Z. Shi, G. Mao, and Y. D. Zhang, "Direction-of-arrival estimation for coprime array via virtual array interpolation," *IEEE Trans. Signal Process.*, to be published, doi: 10.1109/TSP.2018.2872012.

[16] C. Zhou, Y. Gu, Y. D. Zhang, Z. Shi, T. Jin, and X. Wu, "Compressive sensing-based coprime array direction-of-arrival estimation," *IET Commun.*, vol. 11, no. 11, pp. 1719–1724, Aug. 2017.

[17] C. Zhou, Y. Gu, S. He, and Z. Shi, "A robust and efficient algorithm for coprime array adaptive beamforming," *IEEE Trans. Veh. Technol.*, vol. 67, no. 2, pp. 1099–1112, Feb. 2018.

[18] X. Wu, W.-P. Zhu, and J. Yan, "Direction of arrival estimation for off-grid signals based on sparse Bayesian learning," *IEEE Sensors J.*, vol. 16, no. 7, pp. 2004–2016, Apr. 2016.

[19] Z. Yang, L. Xie, and C. Zhang, "Off-grid direction of arrival estimation using sparse Bayesian inference," *IEEE Trans. Signal Process.*, vol. 61, no. 1, pp. 38–43, Jan. 2013.

[20] X. Wu, W.-P. Zhu, J. Yan, and Z. Zhang, "Two sparse-based methods for off-grid direction-of-arrival estimation," *Signal Process.*, vol. 142, pp. 87–95, Jan. 2018.

[21] Z. Yang, L. Xie, and C. Zhang, "A discretization-free sparse and parametric approach for linear array signal processing," *IEEE Trans. Signal Process.*, vol. 62, no. 19, pp. 4959–4973, Oct. 2014.

[22] G. Tang, B. N. Bhaskar, P. Shah, and B. Recht, "Compressed sensing off the grid," *IEEE Trans. Inf. Theory*, vol. 59, no. 11, pp. 7465–7490, Nov. 2013.

[23] Z. Yang, J. Li, P. Stoica, and L. Xie. (2016). "Sparse methods for direction-of-arrival estimation." [Online]. Available: https://arxiv.org/abs/1609.09596

[24] X. Wu, W.-P. Zhu, and J. Yan, "Direction-of-arrival estimation based on Toeplitz covariance matrix reconstruction," in *Proc. IEEE Int. Conf. Acoust., Speech, Signal Process. (ICASSP)*, Shanghai, China, Mar. 2016, pp. 3071–3075.

[25] X. Wu, W.-P. Zhu, and J. Yan, "A Toeplitz covariance matrix reconstruction approach for direction-of-arrival estimation," *IEEE Trans. Veh. Technol.*, vol. 66, no. 9, pp. 8223–8237, Sep. 2017.

[26] Z.-M. Liu, Z.-T. Huang, and Y.-Y. Zhou, "Sparsity-inducing direction finding for narrowband and wideband signals based on array covariance vectors," *IEEE Trans. Wireless Commun.*, vol. 12, no. 8, pp. 1–12, Aug. 2013.

[27] J. Yin and T. Chen, "Direction-of-arrival estimation using a sparse representation of array covariance vectors," *IEEE Trans. Signal Process.*, vol. 59, no. 9, pp. 4489–4493, Sep. 2011.

[28] J. F. Sturm, "Using SeDuMi 1.02, a MATLAB toolbox for optimization over symmetric cones," *Optim. Methods Softw.*, vol. 11, nos. 1–4, pp. 625–653, 1999.

[29] Z. Yang and L. Xie, "On gridless sparse methods for line spectral estimation from complete and incomplete data," *IEEE Trans. Signal Process.*, vol. 63, no. 12, pp. 3139–3153, Jun. 2015.

[30] P. Pal and P. P. Vaidyanathan, "Coprime sampling and the MUSIC algorithm," in *Proc. 14th IEEE DSP/SPE Workshop*, Sedona, AZ, USA, Jan. 2011, pp. 289–294.

[31] Z.-M. Liu, Z. Liu, D.-W. Feng, and Z.-T. Huang, "Direction-of-arrival estimation for coherent sources via sparse Bayesian learning," *Int. J. Antennas Propag.*, vol. 2014, Apr. 2014, Art. no. 959386.

[32] C. Zhou, Z. Shi, Y. Gu, and N. A. Goodman, "DOA estimation by covariance matrix sparse reconstruction of coprime array," in *Proc. IEEE Int. Conf. Acoust., Speech, Signal Process. (ICASSP)*, Brisbane, QLD, Australia, Apr. 2015, pp. 2369–2373.

[33] Z. Shi, C. Zhou, Y. Gu, N. A. Goodman, and F. Qu, "Source estimation using coprime array: A sparse reconstruction perspective," *IEEE Sensors J.*, vol. 17, no. 3, pp. 755–765, Feb. 2017.

[34] M. Grant and S. Boyd, "Cvx: Matlab software for disciplined convex programming, version 1.21," *Global Optim.*, pp. 155–210, 2008.

[35] H. Li, P. Stoica, and J. Li, "Computationally efficient maximum likelihood estimation of structured covariance matrices," *IEEE Trans. Signal Process.*, vol. 47, no. 5, pp. 1314–1323, May 1999.

[36] D. Malioutov, M. Çetin, and A. S. Willsky, "A sparse signal reconstruction perspective for source localization with sensor arrays," *IEEE Trans. Signal Process.*, vol. 53, no. 8, pp. 3010–3022, Aug. 2005.

[37] P. Stoica, P. Babu, and J. Li, "New method of sparse parameter estimation in separable models and its use for spectral analysis of irregularly sampled data," *IEEE Trans. Signal Process.*, vol. 59, no. 1, pp. 35–47, Jan. 2011.

[38] Z. Tan, P. Yang, and A. Nehorai, "Joint sparse recovery method for compressed sensing with structured dictionary mismatches," *IEEE Trans. Signal Process.*, vol. 62, no. 19, pp. 4997–5008, Oct. 2014.

[39] P. Pal and P. P. Vaidyanathan, "A grid-less approach to underdetermined direction of arrival estimation via low rank matrix denoising," *IEEE Signal Process. Lett.*, vol. 21, no. 6, pp. 737–741, Jun. 2014.

XIAOHUAN WU (M'17) received the B.E. and Ph.D. degrees in electrical engineering from the Nanjing University of Posts and Telecommunications, Nanjing, China, in 2010 and 2017, respectively. He is currently a Lecturer with the Nanjing University of Posts and Telecommunications. His research interests include compressed sensing and array signal processing and their applications in millimeter-wave massive MIMO communications.

WEI-PING ZHU (SM'97) received the B.E. and M.E. degrees from the Nanjing University of Posts and Telecommunications, Nanjing, China, in 1982 and 1985, respectively, and the Ph.D. degree from Southeast University, Nanjing, in 1991, all in electrical engineering. He was with the Department of Electrical and Computer Engineering, Concordia University, Montreal, Canada, as a Post-Doctoral Fellow from 1991 to 1992 and a Research Associate from 1996 to 1998. From 1993 to 1996, he was an Associate Professor with the Department of Information Engineering, Nanjing University of Posts and Telecommunications. From 1998 to 2001, he was with hi-tech companies in Ottawa, Canada, including Nortel Networks and SR Telecom Inc. Since 2001, he has been with the Electrical and Computer Engineering Department, Concordia University, as a full-time Faculty Member, where he is currently a Full Professor. Since 2008, he has been an Adjunct Professor with the Nanjing University of Posts and Telecommunications. His research interests include digital signal processing fundamentals, speech and statistical signal processing, and signal processing for wireless communication with a particular focus on MIMO systems and cooperative communication.

Dr. Zhu was the Secretary of the Digital Signal Processing Technical Committee (DSPTC), IEEE Circuits and System Society, from 2012 to 2014, and the Chair of the DSPTC from 2014 to 2016. He served as an Associate Editor for the IEEE TRANSACTIONS ON CIRCUITS AND SYSTEMS PART I: FUNDAMENTAL THEORY AND APPLICATIONS from 2001 to 2003, *Circuits, Systems and Signal Processing* from 2006 to 2009, and the IEEE TRANSACTIONS ON CIRCUITS AND SYSTEMS PART II: TRANSACTIONS BRIEFS from 2011 to 2015. He was also a Guest Editor for the IEEE JOURNAL ON SELECTED AREAS IN COMMUNICATIONS for the Special Issues of Broadband Wireless Communications for High Speed Vehicles, and Virtual MIMO from 2011 to 2013. He is currently an Associate Editor of the *Journal of The Franklin Institute*.

JUN YAN received the Ph.D. degree in electrical engineering from Southeast University, Nanjing, China, in 2012. He was a Visiting Scholar with the Department of Computer and Electronics Engineering, University of Nebraska–Lincoln, Lincoln, in 2014, and a Research Scientist with the Department of Electrical and Computer Engineering, Concordia University, in 2016. He is currently an Associate Professor with the College of Telecommunications and Information Engineering, Nanjing University of Posts and Telecommunications. His research interest is statistical signal processing for wireless location.

ZEYUN ZHANG received the B.E. degree in electronic information science and technology from Shandong University, Jinan, China, in 2005. He is currently pursuing the Ph.D. degree in signal and information processing with the Nanjing University of Posts and Telecommunications, Nanjing, China. His research interests include compressed sensing and array signal processing in radar and communication.

• • •